



**Microenvironment construction of strontium-calcium based biomaterials for bone tissue regeneration: the equilibrium effect of calcium to strontium**

Journal:	<i>Journal of Materials Chemistry B</i>
Manuscript ID	TB-ART-02-2018-000306.R2
Article Type:	Paper
Date Submitted by the Author:	07-Mar-2018
Complete List of Authors:	<p>Xie, Huixu; State Key Laboratory of Oral Diseases, West China Hospital of Stomatology, Sichuan University, Chengdu 610041, China, Department of Head and Neck Oncology Surgery, West China College of Stomatology, Sichuan University</p> <p>Gu, Zhipeng; Sun Yat-Sen University, Department of Biomedical Engineering</p> <p>He, Yan; James Cook University, College of medicine and dentistry</p> <p>Xu, Jia; James Cook University</p> <p>Xu, Chun; e. Oral Health Centre, University of Queensland, Herston, QLD 4006, Australia</p> <p>Li, Longjiang; Sichuan University West China Medical Center, Stomatology</p> <p>Ye, Qingsong; c. College of medicine and dentistry, James Cook University, Cairns, QLD 4878, Australia</p>



## ARTICLE

## Microenvironment construction of strontium-calcium based biomaterials for bone tissue regeneration: the equilibrium effect of calcium to strontium

Received 00th January 20xx,  
Accepted 00th January 20xx

DOI: 10.1039/x0xx00000x

www.rsc.org/

Huixu Xie<sup>a,b,c,†</sup>, Zhipeng Gu<sup>d,†</sup>, Yan He<sup>c,e,†</sup>, Jia Xu<sup>c</sup>, Chun Xu<sup>e</sup>, Longjiang Li<sup>a,b,\*</sup>, Qingsong Ye<sup>c,e,\*</sup>

Strontium-doped calcium phosphate based biomaterials have gained increased recognition for their beneficial effects on bone formation. However, the underneath mechanism is still not clear. In this study, we detected the calcification effects of strontium based materials on osteoblasts *in vitro* and bone formation *in vivo*. The results showed that strontium may inhibit bone cell function in osteoblasts under a standard calcium concentration (1.8 mM) by both reducing alkaline phosphatase activity and inhibiting absorption of osteopontin and osteocalcin. In contrast, a high calcium concentration (9 mM) enhances bone regeneration effect of strontium-based materials. Cultured osteoblasts underwent increased proliferation, calcification and alkaline phosphatase activity when increasing calcium concentrations. An experimental animal model was utilized to simulate a high calcium concentration microenvironment in bone tissue and low calcium concentration in subcutaneous part and the *in vivo* results are similar to the *in vitro* results. These findings suggest that strontium only promoted an anabolic effect on osteoblasts to enhance osteogenesis under a calcium rich microenvironment. Strontium would inhibit bone regeneration under a low dose of calcium *in vivo*. Therefore, strontium seems to be a potentially effective therapeutic option for bone regeneration in combination with a high concentration environment of calcium ion. These results would provide a in-depth knowledge of ion based bone tissue substitute for bone regeneration.

### 1. Introduction

Bone defects that result from congenital, pathological reasons or trauma may severely affect the quality of life. Current clinical treatments of using bone grafts including autografts and allografts have considerable limitations such as inadequate bone amount, secondary surgery etc 1. Bone tissue engineering provides a promising alternative method for the repairing of bone defects and restoring functions, and has emerged as an important area in biomedical engineering 2. Various inorganic biomaterials which contains calcium, phosphate have received great attention due to

their composition similarity to natural bones and great osteoconductivity 3. For example, calcium polyphosphate (CPP), as one class of calcium orthophosphate, is a promising biomaterial in bone regeneration for its comparable physicochemical properties, controllable degradability and excellent biocompatibility 3, 4.

In recent years, strontium has attracted increasingly interests for bone tissue engineering. Strontium is recognized to enhance the proliferation of preosteoblastic cells and stimulate bone formation *in vitro* 5, especially when combined with CPP and hydroxyapatite. In addition, there were significant increases in values of alkaline phosphatase activity and considerably reduced values of osteoclast proliferation using strontium in the existence of calcium. It has also been found that the release of strontium from strontium-doped calcium polyphosphate (SCPP) during degradation of materials supported growth of osteoblastic cells and endothelial cells 6, 7. The effects of strontium ions on growth, dissolution of hydroxyapatite and on bone mineral stimulated proliferation and differentiation of osteoblasts *in vitro* and induced *in vivo* osteoconductivity 8.

However, Wornham et al. reported that strontium itself showed inhibition on the proliferation of osteoblasts and also their mineralization ability 9, which was against previous understandings that Sr<sup>2+</sup> is a promoter of bone formation 10. The study indicated that strontium's role as an agent 'uncouples' bone formation and resorption, where Sr<sup>2+</sup> acts as a global inhibitor of bone cell function 9. Indeed, it had long been assumed that strontium promotes an anabolic effect on osteoblasts and an anti-catabolic effect on

<sup>a</sup> State Key Laboratory of Oral Diseases & National Clinical Research Center for Oral Diseases & Other Research Platforms, Sichuan University, Chengdu 610041, China  
Corresponding author Email: [lilongjiang63@126.com](mailto:lilongjiang63@126.com)

<sup>b</sup> West China School of Stomatology, Sichuan University, Chengdu 610041, China

<sup>c</sup> JCU-WMU Joint Research Group of Tissue Engineering, School of Stomatology, Wenzhou Medical University, Wenzhou, Wenzhou, 325000, China.  
Corresponding author Email: [qingsongye@hotmail.com](mailto:qingsongye@hotmail.com)

<sup>d</sup> Department of biomedical engineering, School of engineering, Sun Yat-sen University, Guangzhou 510006, China

<sup>e</sup> Oral Health Centre, University of Queensland, Herston, QLD 4006, Australia

<sup>†</sup> These authors contribute equally to this work.

\* Corresponding author

osteoclasts, integrated the strontium ion with bio-glass to prepare strontium bio-glass, and displayed an efficacious choice to bone regeneration<sup>11</sup>. To the preosteoblasts, strontium could promoted the cell numbers without calcium-dose-dependently. Similar effects were observed using strontium concentrations ranging from 1-10 mM<sup>12</sup>. Chattopadhyay et al. found that strontium induced osteoblast proliferation though calcium sensing receptor (CaR) in transfected HEK293 cells<sup>13</sup>. It is strongly suggested that the osteogenesis effects of strontium only happen when combined with suitable calcium ion environment. However, there is no report studying the synergetic effects of strontium and calcium on bone formation.

Herein, we hypothesize that the effects of strontium in bone regeneration are related to the concentration of calcium. In this study the osteogenesis effects of strontium together with different concentrations of calcium was evaluated both *in vitro* and *in vivo*. The proliferation, minimization and osteo-related protein expression of osteoblasts were also tested, and to create a model for the application of strontium at different concentrations of calcium.

## 2. Material and methods

### 2.1 Reagents

Fetal calf serum (FBS), Alpha-modified essential medium ( $\alpha$ -MEM) and Trypsin EDTA were obtained from Gibco (Paisley, UK), and strontium chloride and calcium chloride were obtained from Sigma-Aldrich. Other reagents were obtained from Sigma-Aldrich, except where otherwise stated.

### 2.2 Preparation of porous CPP and S CPP scaffolds

We created a microenvironment *in vivo* using the porous scaffolds with or without strontium according to the method used in our previous investigations<sup>4,7</sup>. Briefly, calcium polyphosphate (CPP) and doped strontium calcium Polyphosphate (SCPP) scaffolds were synthesized by gravity sintering. The  $\text{CaCO}_3$  powders was mixed with  $\text{SrCO}_3$  with a molar ratio of Ca/Sr = 92/8, which was the constitution of SCPP. The mixture was added slowly into the phosphoric acid and made the pH reached to 7. These powders were calcined to form molten CPP or SCPP, and the amorphous CPPs or SCPPs were the ball milled and press-formed as a cylinder of 10 mm diameter and 1 mm thickness after being mixed with stearic acid which was the porogen

### 2.3 Calcium-strontium microenvironment for cell culture

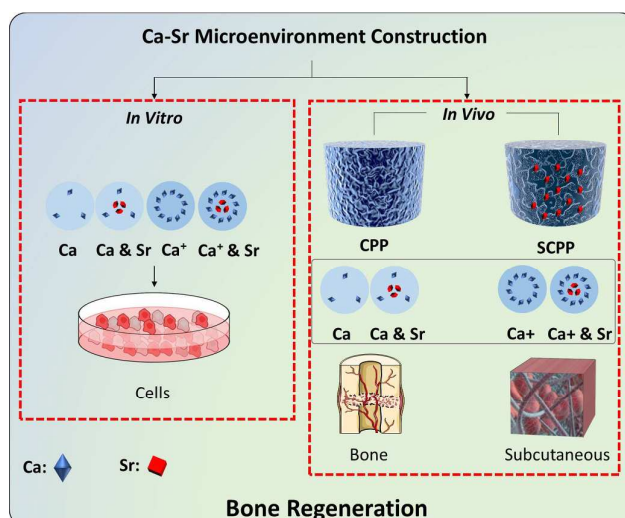


**Figure 1.** Schematic flow chart of experimental design: analyse the effect of bone regeneration under different calcium and strontium microenvironments *in vitro* and *in vivo*.

MC3T3-E1 cells were purchased from American Type Culture Collection (ATCC). Cells were cultured in  $\alpha$ -MEM (GE Healthcare, Chicago, USA) containing 10% fetal bovine serum (FBS, Hyclone, Rockford) and 1% penicillin/ streptomycin and grown at 37 °C with 5%  $\text{CO}_2$ . Cells were plated in 25  $\text{cm}^2$  flasks to harvest when cells reached 60-70% confluence. Cells were plated in 6-well plates for 2, 4, 6, 8 and 16 days in the absence or presence of 1 mM strontium chloride and 1.8 mM or 9 mM calcium chloride, with half medium changes every 3 days. With respect to different concentrations of ions, we established four groups: Group Ca (normal calcium of 1.8 mM), Group Ca&Sr (normal calcium of 1.8 mM and 1 mM strontium), Group Ca<sup>+</sup> (high calcium of 9 mM) and Group Ca&Sr (high calcium of 9 mM and 1 mM strontium). Medium pH,  $\text{pO}_2$  and  $\text{pCO}_2$  were controlled throughout (Fig. 1).

### 2.4 Analysis of cytotoxicity and proliferation of the MC3T3-E1 cells by MTT assay

Cell proliferation was analyzed to test the proliferative rate under different concentrations of  $\text{Sr}^{2+}$  and  $\text{Ca}^{2+}$  by MTT (3-[4, 5-dimethylthiazol-2-yl]-2, 5-diphenyltetrazolium bromide).  $2 \times 10^3$  preosteoblasts were seeded in 96-well plates after overnight cultured (100  $\mu\text{l}$  per well). The cells were cultured for 24 hours, then the supernatant was discarded and the cell culture medium containing various concentration of  $\text{Sr}^{2+}$  and  $\text{Ca}^{2+}$  were added to the MC3T3-E1 cells on the basis of equal surface areas into each well ( $n = 6$ ). The plates were detected on the second, fourth, sixth and eighth day respectively. 10  $\mu\text{l}$ /well MTT solution (5 mg/ml in test medium) was added in by using multichannel pipetting gun, and then the plate was incubated for a further 4h at 37 °C. Dimethylsulfoxide (150  $\mu\text{l}$ /well) was instilled into wells then the plates were shaken in the shaking bed for 10 minutes. The optical density (OD) value of each well was test by a microplate reader (Model550, Bio Rad Corporation) at a wavelength of 490 nm to evaluate preosteoblasts number.

## 2.5 Alizarin red staining

Alizarin red staining (ARS) of MC3T3-E1 osteoblasts was conducted to detect the ability of binds selectively to calcium salts. Briefly, MC3T3-E1 osteoblasts were seeded in a 12-well plates ( $5 \times 10^3$  cells, 1 ml per well). At the pre-set time points (2, 4, 8 and 16 days), MC3T3-E1 osteoblasts were rinsed with PBS solution, then fixed with 0.5 ml formaldehyde (10%) at room temperature for 20 minutes, washed three times with distilled water and stained with 1 ml of ALR solution (15 mg/ml, pH 4.2) at room temperature for 60 minutes. The plates were air dried for 24 hours. Images of entire individual wells of ALR stained cells were obtained using XX microscopy (40X objective). To quantify ALR staining, stained cultures were destained by using 10% (w/v) cetylpyridinium chloride (CPC) for 30 minutes at room temperature. The resulting solutions were read on a microplate reader (Ascent) with a test wavelength of 562 nm. Measurements were carried out in three separate wells.

## 2.6 Determination of alkaline phosphatase (ALP) activity

All procedures were performed using MC3T3-E1 grown for 2, 4, 6 and 8 days according to the manufacturer's protocol (Alkaline Phosphatase [ALP] Fluorometric Assay kit; Abcam, Cambridge, MA). Briefly, necessary amounts of cells were harvested for each assay ( $1 \times 10^5$  cells), cells washed with cold PBS and resuspended in 110  $\mu$ l of assay buffer. Cells were homogenized quickly by pipetting up and down a few times and centrifuged for 3 minutes at 4 °C with 13,000 rpm using a cold micro-centrifuge to remove any insoluble material. Supernatant was collected and transferred to a clean tube, and added to each well of a Fluotrac 96-well plate (Corning, NY). Methylumbelliferyl phosphate disodium salt (20  $\mu$ l, 0.5 nM Abcam) substrate was instilled to each well, co-cultured for 30 minutes at 25 °C, and then stop the reaction through adding 20  $\mu$ l of stop solution to each well. Fluorescence intensity was measured at 360 nm for excitation and 440 nm for emission by using a fluorescence microplate reader (POLARstar Omega, BMG LABTECH, Offenburg, Germany). Enzyme activity was calculated: ALP activity =  $A/V/T$  (mU/ml), where A is the amount of 4-MU generated by samples (in nmol), V is the volume of sample added in the assay well (in ml) and T is the reaction time (in minutes). All experiments were independently performed three times in triplicates.

## 2.7 Enzyme-linked immunosorbent assay (ELISA) for Osteocalcin & Osteopontin Expression

The concentrations of osteocalcin (OCN) and osteopontin (OPN) in cell-conditioned culture medium and cells were determined by means of enzyme-linked immunosorbent assay (ELISA) kits (SimpleStep ELISA™ Kit, Abcam, Cambridge, MA) according to the manufacturer's instructions. All experiments were independently performed three times in triplicates. Briefly, centrifugation of cell culture media at 2,000 rpm for 10 minutes was undertaken to remove debris and collect supernatants and assay. The necessary amount of cells were harvested for each total protein assay (105 cells), the suspension centrifuged at 1,500 rpm for 10 minutes at 4 °C and the supernatant aspirated. The pellet was suspended in cold PBS, transferred to a TPX tube and centrifuged at 1,500 rpm for 10 minutes at 4 °C. Using the 1X Cell Extraction Buffer PTR, the protease inhibitor (Abcam, Cambridge, MA) was added to the ice-cold cell lysis buffer. The buffer was then added and the pellet

suspended and incubated on ice for 10 minutes. Completion of extraction was at 5 cycles. The supernatant was transferred to a new tube and the samples centrifuged at 14,000 rpm for 15 minutes at 4 °C to remove any remaining insoluble material. An aliquot was used for undertaking quantification. Protein extracts were stored at -80 °C. A volume of 50  $\mu$ l of all sample or standard was added to appropriate wells, 50  $\mu$ l of the antibody cocktail added to each well, then incubated for 1 hour on shake cultivation. After 1 hour, each well was washed with adequate 1X Wash Buffer, then 100  $\mu$ l of TMB Substrate added to each well and incubated for 10 minutes in the dark. In the end, 100  $\mu$ l Stop Solution was instilled with 1 minute mixing to stop the reaction. The results were read on a microplate reader (Ascent) with a test wavelength of 450 nm. Measurements were carried out in three separate wells.

## 2.8 Calcium-strontium microenvironment for animal study

All animal experiment procedures were approved by Animal Ethics Committee of West China Hospital of Stomatology, Sichuan University. The animals were used according to institutional guidelines. Firstly, we detected calcium environments in various positions of bone, muscle and subcutaneous regions. We found the calcium concentration in muscle and skin approximating 2 mM, and in bone defect regions around three times higher. These were consistent with values reported previously in the literature. Eighteen healthy New Zealand white rabbits weighing about  $2.2 \pm 0.2$  kg each were anesthetized with pentobarbital sodium. To construct the microenvironment in vivo, Porous CPP and SCPP scaffolds was used as the bone regeneration scaffolds for animal experiments were prepared according to methods described by previous studies<sup>14</sup>. For subcutaneous and intramuscular implantation, chose a piece of skin was prepped, sterilized with iodine, then make the parallel lengthwise incision on each animal's back. The pocket incision was cut near to the spinal column to make a small pouch where the scaffold implanted. For bone implantation, an approximately round defect ( $\phi = 10$  mm) above the skull was filled with the prepared scaffold with  $\phi = 10$  mm. Each group of animals were sacrificed on pre-set time point at 4 weeks, 8 weeks and 12 weeks, respectively. The scaffolds with surrounding tissue were en bloc resection, and the whole tissues were fixed, decalcified and embedded in paraffin following the standard procedure. The samples were sectioned and stained with hematoxylin and eosin (H&E), then observed using a light microscope (Zeiss, Germany).

The immunohistochemical procedures employed were introduced in a previous study. Anti-MMP2, anti-VEGF, anti-OPN and anti-OCN were purchased from Sigma-Aldrich, and the IHC Select® Immunoperoxidase Secondary Detection System (Millipore, Germany) had been applied according to the manufacturer's instructions. Briefly, endogenous peroxidase activity was blocked by incubation with hydrogen peroxi (pH 8.0), boiled in high temperature steam for 1 minute, and allowed to cool. Two drops of the blocking reagent were applied to the specimen for 5 minutes, followed by the addition of two drops of the primary antibody- or a negative control reagent- to the samples 10 minutes. Under the IHC Select® system, biotin-conjugated secondary antibody was instilled 10 minutes, incubated with streptavidin HRP 10 minutes, added a fresh DAB solution 10 minutes, then stained with hematoxylin counter stain solution 1 minute in the end. After staining, each section was observed under a light microscope (100 X magnification)

## ARTICLE

and at 10 different locations randomly selected. All analyses were repeated at least three times by two independent investigators on blinded samples. Using image analytical software Image-ProPlus (Media Cybernetics, USA), new bone volume was expressed as the percentage of newly formed bone area in the available pore space (bone area/pore area  $\times$  100%).

## 2.9 Statistical analysis

The data were analysed with SPSS version 19.0 (IBM Corp., Armonk, NY). *T*-tests or analyses of variance (ANOVA) were used to test categorical variables. Statistical significance was determined by a *p* value below 0.05.

## 3. Results

### 3.1 Strontium inhibits bone regeneration with low dose calcium and promotes bone regeneration with high dose calcium in vitro

It had been indicated that  $\text{Sr}^{2+}$  play the role of enhancing bone cell proliferation and bone formation combined with  $\text{Ca}^{2+}$  in vitro<sup>14,15</sup>. However, several early studies have suggested that  $\text{Sr}^{2+}$  inhibited biomineralization when co-cultured with rat osteoblasts<sup>9</sup>. Fig. 2A&B shows the cytotoxicity results of different concentrations of calcium with or without strontium. The OD values showed that the cell proliferation changed with culture time for the four groups. The growth rate was group  $\text{Ca+Sr} > \text{Ca+} > \text{Ca} > \text{Ca&Sr}$  during the entire culture period. Continuous treatment with strontium salts under low calcium concentration caused cell number reduction of preosteoclasts in 8-day old cultures. However, continuous treatment with strontium salts under high calcium concentrations promotes the proliferation of osteoclast significantly. A moderate reduction of osteoblast ALP activity was observed in 8 day old cultures treated with  $\text{SrCl}_2$  under low calcium concentration. In parallel, strontium salts caused increases in ALP activity under high calcium concentrations. To determine the most effective and consistent protocol for osteoblast differentiation, the MC3T3-E1 was used. The osteogenic differentiation potential of MC3T3-E1 was assessed based on Alizarin Red and Toluidine Blue staining, in order to detect deposition of calcium nodules, immunohistochemistry of sphere formation and secretion of osteogenic-specific OPN and OCN under our culture conditions.

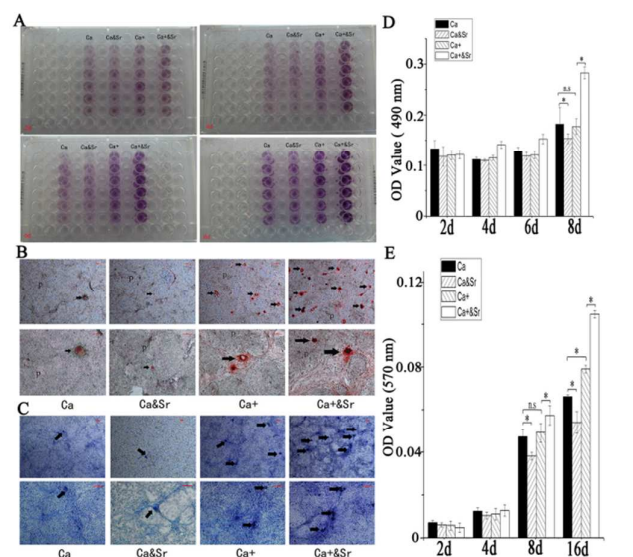


**Figure 2.** Osteogenesis differentiation ability of Ca/Sr ions on MC3T3-E1 cells.

A: MTT assay for proliferation of MC3T3-E1 in different concentration of Ca/Sr ions;

B: Quantitative analysis of MTT (\**p* < 0.05; n.s: no statistically significance);

C: Osteogenesis was assessed by staining cultures with Alizarin Red to detect the formation of mineralized nodules (c: osteoblast cells regions; p: pre-calcification regions; t: tube-like structure; black arrow: calcification nodules); red bar: 100  $\mu$  m.

D: Semiquantitative analysis of Alizarin Red staining of Ca/Sr ions on MC3T3-E1 cells. (\**p* < 0.05; n.s: no statistically significance);

E: Toluidine blue staining results of Ca/Sr ions on MC3T3-E1 cells. The formation of calcification nodules was indicated by black arrows. red bar: 100  $\mu$  m.

To develop an acid extraction protocol for the extraction and quantification of Alizarin Red S, MC3T3-E1 cells were prepared in 25  $\text{cm}^2$  flasks in dexamethasone-free medium. As the simplest and easiest approach, MC3T3-E1 cells were directly plated into 12-well plates. Robust osteoblast differentiation was determined by ARS staining (Fig. 2C). On staining of the monolayers with ARS, a deep stained mineralized layer was evident. Strontium caused a significant promotion of mineralisation with high dose calcium at a concentration of 9 mM. At calcium chloride concentrations of 1.8 mM, with or without strontium chloride, inhibition of mineralisation was elicited of control values. On day 8, MC3T3-E1 cells gradually produced dye-stained mineral appearing as dense nucleation points that expanded over the entire monolayer. Pre-osteoblasts differentiated in group  $\text{Ca+Sr}$  and  $\text{Ca+}$  significantly, with large amounts of pre-calcification regions observed. Little to no osteoblast differentiation in group  $\text{Ca}$  and  $\text{Ca&Sr}$  was observed, as indicated by ARS staining on day 8. Osteoblast differentiation in group  $\text{Ca+Sr}$  was increased at culture day 16 when compared to group  $\text{Ca+}$ . Osteoblast differentiation in group  $\text{Ca}$  was increased at

culture day 16 when compared to group Ca&Sr. After 16 days of treatment with 1 mM strontium under high calcium concentration, mineralization was increased in 16-day cultures of osteoblasts, where many calcification nodules were observed and appeared as deep red features. However, after 16 days of treatment with 1 mM strontium under low calcium concentration, corresponding phase contrast micrographs showed few calcification nodules and unstained cell layers, and calcification nodules appeared as slight red or white-grey features. ARS staining of the 12-well plates was quantified using CPC extraction, and the absorbance of ARS was measured at 562 nm. Semi-quantitative analysis of ARS staining revealed that the cells treated with group Ca+&Sr produced significantly higher stained mineral than other groups ( $p < 0.05$ ) (Fig. 2D). There was a statistic difference between each group, and the OD values were Ca+&Sr ( $0.105 \pm 0.001$ ) > Ca+ ( $0.079 \pm 0.002$ ) > Ca ( $0.054 \pm 0.005$ ) > Ca&Sr ( $0.066 \pm 0.001$ ) at culture day 16. On staining of the monolayers with Toluidine Blue, the same trend as demonstrated with the use of ARS was observed. Many calcification nodules were observed and appeared as deep blue features in Ca+&Sr (Fig. 2E).

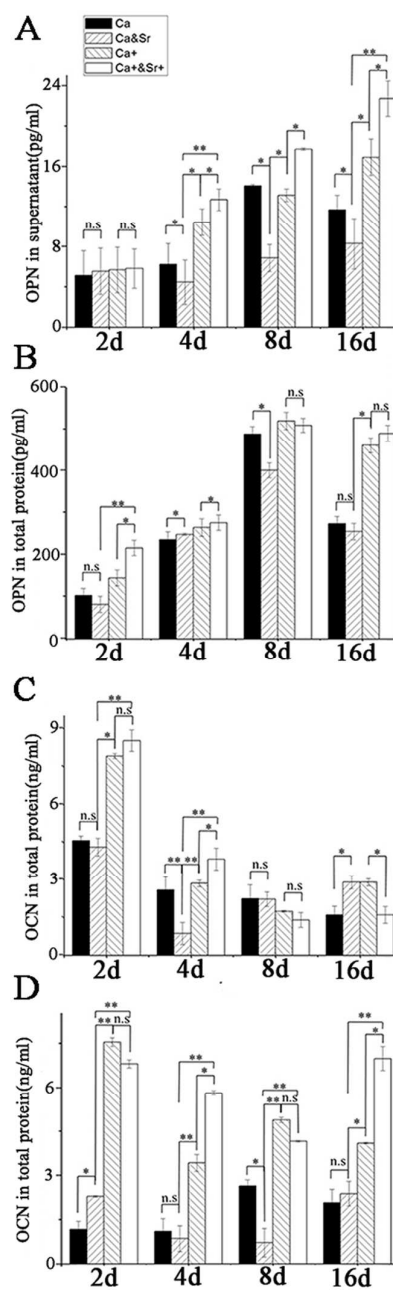


**Figure 3** Expression of OPN and OCN in pre-osteoblasts detected by ELISA in each group (\* $p < 0.05$ ; \*\* $p < 0.01$ ; n.s: no statistically significance).

The protein expression of OPN in total protein and supernatant in cells treated with group Ca+&Sr and Ca&Sr had the highest and lowest OPN concentrations in supernatant among the groups at 4 days, 8 days and 16 days, respectively ( $p < 0.05$ ). OPN concentration in total protein showed the same trend as in supernatant at 8 days and 16 days. However, there were no statistically significant differences in protein expression of OPN in total protein between the groups treated with Ca+&Sr and Ca+ or the groups treated with Ca&Sr and Ca (Fig. 3A, B). It was difficult to summarise the trends of



the expression of OCN protein in preosteoclasts, however, OCN in total protein and supernatant decreased gradually which culminated in a time point of 2 days. High expression of OCN protein was significantly associated with high calcium concentration (group Ca+&Sr and group Ca+) (Fig. 3C, D). These data indicated that strontium increased the osteoblast differentiation and mineralisation with high calcium concentrations, but may have not promoted differentiation and mineralisation with low calcium concentrations *in vitro*.

### 3.2 SCPP promotes bone regeneration under high dose calcium environment *in vivo*

In intramuscular and subcutaneous experiments, all surgery operations were completed successfully without operation related complications. Without any the implanted sites on the rabbits showed infection and inflammation sign in local regions after the operations. All implanted sites were covered by normal tissue and all scaffolds' integrity in appearance were maintained. Tissue biopsies evaluation of the scaffolds and implanted surrounding tissues demonstrated differences in responses (Fig. 4). In SCPP groups, the interface between scaffolds and surrounding tissues was clearly distinguishable after implantation at 12 weeks. The scaffolds and implanted surrounding tissues showed the classic structure of large fibrous filled implanted SCPP scaffolds in subcutaneous implant regions. Here, the presence of sporadic and little amounts of osteoid around the margin of scaffolds and subcutaneous tissues were detected on pre-set 12 weeks time point. In CPP groups, a few amounts of new fibrous tissue formed in the scaffolds and little fibrous areas in the center of the scaffolds. The interfaces between scaffolds and subcutaneous tissues were indistinct after 12 weeks. A layer of osteoid could be observed around the margin of scaffolds, while phagocytosis displayed by light microscopy were not observed during the duration of the entire observe period. During the 12 weeks' analysis period, ectopic bone formations were observed in both groups, however the amount of osteoid was larger in group CPP than that with SCPP.

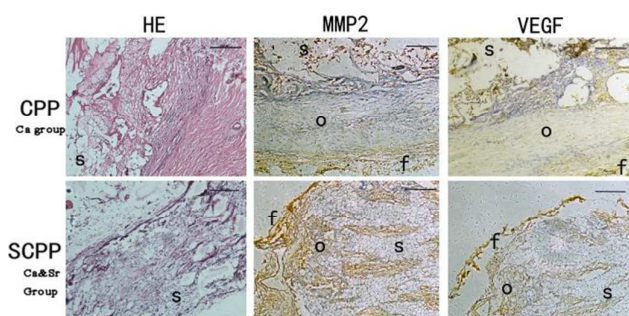


**Figure 4.** Images of histological sections of CPP and SCPP scaffolds after 12 weeks of subcutaneous implantation with H&E staining (o: osteoid; f: fiber tissue; s: scaffolds). Black bar:100  $\mu$  m.

Fig. 5 shows tissue biopsies evaluation photographs of SCPP and CPP scaffolds after scaffolds implantation in muscle pouches during for the 12 weeks' observe period. Every implanted site was covered by muscle tissue, and scaffolds were not observable. The foreign body reactions (FBR) in either CPP or SCPP implants were innocuous, similar to intramuscular regions. In SCPP groups, the interface between scaffolds and surrounding tissues were still

distinct after implantation at 12 weeks. The SCPP scaffolds and surrounding tissues showed the typical structure of fibrous tissue around the scaffolds, with the presence of small amounts of osteoid. In CPP groups, small amounts of new fibrous tissue formed in the scaffold, and muscle cells become as specialized as osteoid. The interfaces between scaffolds and intramuscular tissues were not clearly visible after implantation at 12 weeks. A layer of osteoid could be observed around the margin of scaffolds, while phagocytotic activity was not observed during the entire study period. During the 12 weeks, ectopic bone formation was observed in both groups, with higher osteoid amount in CPP group.

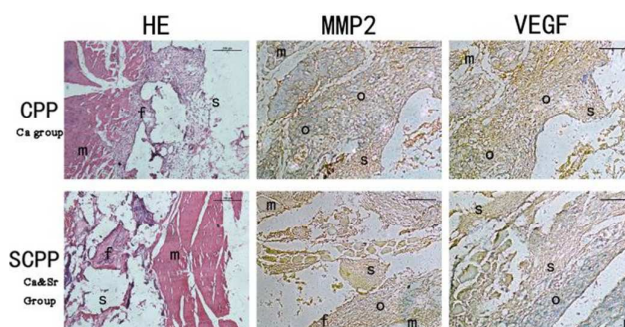


**Figure 5.** Images of histological sections of CPP and SCPP scaffolds after 12 weeks of intramuscular implantation with H&E staining (o: osteoid; f: fiber tissues; s: scaffolds; m: muscle tissues). Black bar:100  $\mu$  m.

After 4 weeks of scaffolds implantation, new formed bone penetrated through the inter-connective multiholes to the centre of the scaffolds. The boundary among scaffolds and main host bone were hardly detected in SCPP group, associated with a close union formed without any gap. The new bulky areas of new formed bone in the centre of the scaffolds, with trabecular structure encasing the scaffold, were consistently seen. In the case of the CPP group, host bone formed a close union while the new bone regenerated and penetrated through the inter-connective multiholes in the margin. While in the center of the remaining scaffolds region, no newly formed bone or degradation residue of CPP scaffolds were detected (Fig. 6A).

Primarily, the amounts of newly formed bone in SCPP group increased dramatically, much higher than that of the CPP scaffolds after implantation at 8 weeks. OPN and OCN positive cells (osteoblasts) were observed in the center of the scaffolds of SCPP and the newly formed bone structures around positive cells in SCPP group. While it was not easy to find the positive cells in the centre of CPP scaffolds, and more fibers were observed in the porous space of CPP scaffolds. Between 8 weeks and 12 weeks, the formation rate of newly formed bone in SCPP group slowed down, while CPP group still keep stable. These results showed that SCPP scaffolds presented higher efficiency of bone formation than CPP scaffolds during the observe period (Fig. 6B). To quantitatively analysis the amount and rate of newly formed bone, we calculated the volume of newly formed bone. The amounts of newly formed bone in SCPP group were more than CPP group, and the rate was much higher than that of the CPP scaffolds before 8 weeks. After that period, the rate of bone formation in SCPP group slowed down, while that rate in CPP group keeps stable. However, the amounts of newly formed bone in SCPP group were more than CPP group in

whole study period. These results had been shown that SCPP scaffolds presented a higher efficiency of bone formation than CPP scaffolds in the long term (12 weeks analysis period) (Fig. 6C).

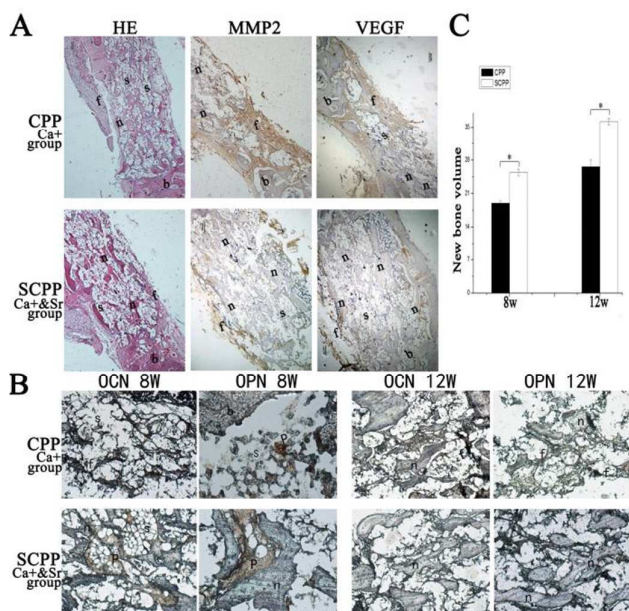


**Figure 6.** A: Histological observation of CPP and SCPP scaffolds after 12 weeks of bone implantation (f: fiber tissues; s: scaffolds; b: bone of original; n: new bone) Black bar:100  $\mu$  m.

B: Immunohistological results of OPN and OCN expression with CPP and SCPP scaffolds after 8 weeks and 12 weeks' implantation (f: fiber tissues; s: scaffolds; b: bone of original; n: new bone; p: positive cells)

C: Quantification of newly formed bone. Error bars represent means  $\pm$  SD (n = 3).

#### 4. Discussion

In recent years, strontium's efficacy has been increasingly recognized as a function of baseline fracture risk. A meta-analysis in terms of strontium ranelate reported that strontium could play important role in decreasing the risk of kinds of clinical fractures<sup>16</sup>. However, the mechanisms by which strontium exerts its effects on bone and how to use strontium suitably have remained unclear<sup>17</sup>. Our results clearly demonstrated that strontium's effects on bone formation depended on the concentration of calcium. Here, strontium inhibited bone regeneration under a low dose of calcium, and promoted bone regeneration under a high dose of calcium *in vitro* and *in vivo*.

Like calcium, strontium is a divalent cation, and has been routinely administered as an anti-osteoporotic drug that can keep the balance between bone resorption and bone formation. Strontium is indicated for use in postmenopausal women and men<sup>18</sup>. Strontium was accounted for significantly increases the bone mineral density, with an annual increase in bone mineral density of 2.9% when administering 2 g/day of strontium ranelate<sup>17,19</sup>. To make clear the mode of action of strontium, there were a lots of detailed *in vivo*

studies focusing on kinds of factors, such as dose, plasma strontium levels and the site of accumulation in the skeleton<sup>20</sup>. The relation between dose and femoral strontium levels in a rat model was considered to a strong and linear correlation, where higher doses have shown a diminishing effect, possibly due to saturation of the gastrointestinal mechanisms of absorption<sup>20</sup>. Furthermore, plasma strontium levels have shown a similar effect. Strontium absorption takes place in the gastrointestinal tract and occurs *via* an active mechanism involving a protein that binds calcium. Having been taken up in the gut and concentrated in the bone, strontium is then excreted almost entirely in the urine *via* the kidneys. Following withdrawal of administration of strontium at six weeks, bone levels of strontium have been reported to be 50%, with the remaining strontium concentrated. Strontium has been shown to increase preosteoblastic proliferation in a rat calvarial model, and can promote the activity of functionally mature cells to stimulate bone matrix synthesis<sup>21</sup>.

Wornham et al. demonstrated that strontium salts had direct effects on bone cell function *in vitro*, with  $\text{Sr}^{2+}$  acting as an inhibitor of bone cell function and with particularly marked effects on biomineralization<sup>9</sup>. However, we found that the authors neglected a key point: the performances of concentration of strontium and calcium in a biological microenvironment were essential for guiding their biomedical applications<sup>22</sup>. The focus should be on the concentration of the two ions. In one study, Marie et al. demonstrated that SrR at clinically relevant doses prevented bone loss in ovariectomized rats, by reducing bone resorption and maintaining bone formation. Some studies indicated that the strontium could partially slowdown trabecular bone loss in estrogen-deficient rats model, with the beneficial effects on bone mass in osteopenic disorders<sup>23</sup>. Acute stimulation of proliferation of rat osteoblasts has been previously described following exposure to high concentrations (1-5 mM) of SrR. Motivated biomineralization with expression increase of alkaline phosphatase mRNA were observed through mouse osteoblasts treated chronically with 0.1-1 mM strontium<sup>9</sup>. Therefore we used 1 mM strontium to affect preosteoblasts. Another key problem of our study was confirming the concentration of calcium. The formulation of the standard DMEM cell culture medium contains calcium at a concentration of 1.8 mM. This calcium is required for the mineralisation evident in our control cultures, consistent with the concentration of calcium in normal blood and interstitial fluid. However, it is difficult to detect the concentration of effective calcium around bone. Sugimoto et al reported that a high concentration of extracellular calcium stimulated osteoblastic MC3T3-E1 cells when cultured at high calcium concentrations (more than 3 mM). The present study had been shown that an increase in extracellular calcium could stimulate the DNA synthesis and ALP activity of osteoblasts, indicating the importance of high  $\text{Ca}^{2+}$  concentrations at the resorptive sites in bone remodelling<sup>24</sup>. D'Haese et al measured trace elements in the bone of patients with end-stage renal disease and we estimated the concentration of calcium in bone to be approximately 5-10 mM. In this study, we considered a high calcium concentration to be 9 mM<sup>25</sup>.

The findings of this study showed a promoting effect of strontium chloride to ALP activity, and further, calcification of osteoblasts under high calcium concentrations *in vitro*. High concentrations of strontium caused proliferation of rat osteoblasts. Other studies have also shown that increased calcification and expression of alkaline phosphatase mRNA were observed in mouse osteoblasts



treated with 1 mM strontium<sup>26</sup>. Also demonstrated in this study was an inhibition effect of strontium chloride to alkaline phosphatase activity and calcification of osteoblasts under low calcium concentrations *in vitro*. These findings correspond with the results of Wornham et al. that suggests strontium acts as an inhibitor of bone cell function with particularly marked effects on biomineralization. These results explain the significant component of increased bone mineral density measured in strontium-treated patients, and may be due to the incorporation of strontium which has more than twice the atomic mass of calcium<sup>27</sup>. We set up a rabbit model to verify the results *in vitro*. We made a critical defect in the calvarial bone of rabbits which indicated high concentration calcium environments, and at the same time made an intramuscular and subcutaneous implantation which represented the high concentrations of low calcium environments *in vivo*. Our results supported the hypothesis that strontium's double-faced behaviour towards bone regeneration was related to the concentration of calcium *in vivo*. Recent work has been set up effectively in a range of apatite-based glasses doped with strontium<sup>28,29</sup>. In our previous research, *in vivo* studies have been shown that SCPP with a proper dose of strontium had the potential to promote the formation of angiogenesis and the bone regeneration.

## Conclusions

Overall, we concluded that strontium's dual behaviour towards bone regeneration was related to the concentrations of calcium. We found that strontium inhibited bone regeneration under a low dose of calcium, and promoted bone regeneration under a high dose of calcium. Our work contributes to the understanding of the mechanisms of action of strontium on bone forming.

## Conflicts of interest

There is no conflict of interest among the authors.

## Acknowledgements

We sincerely acknowledge the funding and generous support of the National Natural Science Foundation of China (No. 51641305) and youth fund of Sichuan University and West China School of Stomatolog and the fund of Australia Research Council(DE120101666). The authors would like to thank Dr. Christopher Franco from James Cook University for his kind help in the manuscript preparation.

## References

1. R. J. O'Keefe and J. Mao, *Tissue Engineering Part B Reviews*, 2011, **17**, 389-392.
2. J. P. Vacanti and R. Langer, *Lancet*, 1999, **354 Suppl 1**, S32-S34.
3. S. Bose, G. Fielding, S. Tarafder and A. Bandyopadhyay, *Trends in biotechnology*, 2013, **31**, 594-605.
4. H. Xie, J. Wang, C. Li, Z. Gu, Q. Chen and L. Li, *Ceramics International*, 2013, **39**, 8945-8954.

5. J. Zhang, S. Zhao, Y. Zhu, Y. Huang, Z. Min, C. Tao and C. Zhang, *Acta biomaterialia*, 2014, **10**, 2269-2281.
6. D. Gopi, S. Ramya, D. Rajeswari and L. Kavitha, *Colloids & Surfaces B Biointerfaces*, 2013, **107**, 130-136.
7. Z. Gu, B. Huang, Y. Li, M. Tian, L. Li and X. Yu, *Materials Science & Engineering C*, 2016, **61**, 526-533.
8. H. Zreiqat, Y. Ramaswamy, C. Wu, A. Paschalidis, Z. F. Lu, B. James, O. Birke, M. McDonald, D. Little and C. R. Dunstan, *Biomaterials*, 2010, **31**, 3175-3184.
9. Wornham DP, Hajjawi MO, Orriss IR and A. TR., *Osteoporos Int*, 2014, **25**, 2477-2484.
10. Z. Gu, H. Wang, L. Li, Q. Wang and X. Yu, *Biomedical Materials*, 2012, **7**, 065007.
11. E. Gentleman, Y. C. Fredholm, G. Jell, N. Lotfibakhshaiesh, M. D. O'Donnell, R. G. Hill and S. Mm., *Biomaterials*, 2010, **31**, 3949-3956.
12. J. Caverzasio, *Bone*, 2008, **42**, 1131-1136.
13. Chattopadhyay N, Quinn SJ, Kifor O, Ye C and B. EM., *Biochem Pharmacol.*, 2007, **74**, 438-447.
14. Qiu K, Zhao XJ and e. a. Wan CX, *Biomaterials*, 2006, **27**, 1277-1286.
15. Z. Gu, H. Xie, L. Li, X. Zhang, F. Liu and X. Yu, *Journal of Materials Science: Materials in Medicine*, 2013, **24**, 1251-1260.
16. J. Kanis, *Osteoporosis International*, 2014, **22**, 2347-2355.
17. M. D. Patrick Ammann, I. Badoud, S. Barraud, R. Dayer and R. Rizzoli, *Journal of Bone & Mineral Research*, 2007, **22**, 1419-1425.
18. N. J. Lakhkar, I.-H. Lee, H.-W. Kim, V. Salih, I. B. Wall and J. C. Knowles, *Advanced drug delivery reviews*, 2013, **65**, 405-420.
19. C. Roux, J. Fechtenbaum, S. Kolta, G. Isaia, J. B. Andia and J. P. Devogelaer, *Annals of the Rheumatic Diseases*, 2008, **67**, 1736-1738.
20. S. G. Dahl, P. Allain, P. J. Marie, Y. Maura, G. Boivin, P. Ammann, Y. Tsouderos, P. D. Delmas and C. Christiansen, *Bone*, 2001, **28**, 446-453.
21. M. B. Camargo, T. Vilaça, L. F. Hayashi, O. G. Rocha and M. Lazaretti-Castro, *Journal of Bone & Mineral Metabolism*, 2014, **33**, 319-328.
22. M. Cattani-Lorente, R. Rizzoli and P. Ammann, *Acta biomaterialia*, 2013, **9**, 7005-7013.
23. H. Xie and Q. Ye, *Osteoporosis International*, 2015, **26**, 2213-2214.
24. I. Kanazawa, T. Yamaguchi, S. Yano, M. Yamauchi, M. Yamamoto and T. Sugimoto, *Bmc Cell Biology*, 2007, **8**, 229-236.
25. P. C. D'Haese, M. M. Couttenye, L. V. Lamberts, M. M. Elseviers, W. G. Goodman, I. Schrooten, W. E. Cabrera and M. E. De Broe, *Clinical chemistry*, 1999, **45**, 1548-1556.
26. E. Bonnelye, A. Chabadel, F. Saltel and P. Jurdic, *Bone*, 2008, **42**, 129-138.
27. G. M. Blake and I. Fogelman, *Journal of Clinical Densitometry*, 2007, **10**, 34-38.
28. M. H. Alkhrasat, F. T. Mariño, C. R. Rodríguez, L. B. Jerez and E. L. Cabarcos, *Acta biomaterialia*, 2008, **4**, 664-670.
29. J. Liu, S. C. Rawlinson, R. G. Hill and F. Fortune, *Dental Materials Official Publication of the Academy of Dental Materials*, 2016, **32**, 412-422.